

Full folding calculations for proton-nucleus elastic scattering at intermediate energies

R. Crespo,* R. C. Johnson, and J. A. Tostevin

Department of Physics, University of Surrey, Guildford, Surrey GU2 5XH, United Kingdom

(Received 11 December 1989)

The full folding optical potential for the elastic scattering of protons from ^{16}O and ^{40}Ca at 200 MeV is calculated. The fully off-shell free nucleon-nucleon t matrix, at a fixed energy, derived from the Paris potential and harmonic oscillator nuclear single-particle wave functions are used for both systems. The calculated observables show that the optimal factorization approximation provides a good description for both nuclei.

I. INTRODUCTION

In this paper we will examine the accuracy of the optimal factorization approximation, compared with the full folding approach, for calculations of the observables of proton elastic scattering from ^{16}O and ^{40}Ca at 200-MeV incident energy. Calculations in similar spirit have also been reported recently by Elster *et al.*,¹ for ^{16}O , and by Arellano *et al.*,² for ^{40}Ca . These calculations differ however, in detail, with each other with regard their physical input. For example, they use different underlying nucleon-nucleon (NN) interactions, different prescriptions for the energy at which the NN transition matrix is to be evaluated and different approximate treatments of the proton-target Coulomb interaction. Furthermore, the calculations appear to disagree on the basic question of the accuracy of the optimal factorization procedure.

Pauli blocking effects must be taken into account in order to understand quantitatively experimental data³ for proton elastic and inelastic scattering at intermediate energies. In finite nucleus calculations at intermediate energies, such effects are naturally taken into account within the Kerman-McManus-Thaler (KMT) multiple-scattering formalism.⁴ The inclusion of higher-order terms in the optical potential is, however, extremely complicated. It

is essential, therefore, to investigate carefully the accuracy of the approximations currently made in the first-order term, in particular the optimal factorization approach,⁵ which might lead to great simplifications in the evaluation of higher-order terms.

For these reasons, in this paper we have undertaken a consistent theoretical treatment of both the ^{16}O and ^{40}Ca systems, which uses the same underlying NN and target structure models. Our calculations also differ from the published works in that they include a more accurate treatment of the proton-target Coulomb interaction. In view of the very significant differences between the predictions of the optimal factorization and full folding calculations, which were introduced by the addition of the Coulomb interaction in the work of Elster *et al.*, it is important to clarify whether this phenomenon might result simply from the rather crude treatment of the Coulomb interaction used in that study.

II. THE FIRST-ORDER OPTICAL POTENTIAL

According to the KMT multiple-scattering formalism, the first-order optical potential for proton-nucleus scattering, in momentum space, is given by the expression

$$\langle \mathbf{k}' | \hat{U}^{(1)} | \mathbf{k} \rangle = \frac{A-1}{A} \sum_{\alpha_i, i=n,p} \langle \mathbf{k}' \alpha_i | t_{0i}(\epsilon) | \mathbf{k} \alpha_i \rangle = \frac{A-1}{A} \sum_{\alpha_i, i=n,p} \int d\mathbf{p} \int d\mathbf{p}' \langle \alpha_i | \mathbf{p}' \rangle \langle \mathbf{k}' \mathbf{p}' | t_{0i}(\epsilon) | \mathbf{k} \mathbf{p} \rangle \langle \mathbf{p} | \alpha_i \rangle, \quad (1)$$

where we have assumed that the target nucleus ground state is described by a single Slater determinant of occupied single-particle wave functions $\{\alpha_i\}$ and the sum, in Eq. (1), runs over all occupied states. Here \mathbf{k} and \mathbf{k}' are projectile momenta in the nucleon-nucleus (NA) center-of-mass frame, and $t_{0i}(\epsilon)$ is the antisymmetrized free nucleon-nucleon transition matrix evaluated at an appropriate relative energy ϵ in the NN center-of-mass frame. Additional effects, arising from the full antisymmetrization of the nucleon-nucleus optical potential, have been shown to be negligible.⁶

Using momentum conservation for the interacting nucleon pair, we write

$$\langle \mathbf{k}' \mathbf{p}' | t_{0i}(\epsilon) | \mathbf{k} \mathbf{p} \rangle = \delta(\mathbf{k}' + \mathbf{p}' - \mathbf{k} - \mathbf{p}) \left\langle \frac{\mathbf{k}' - \mathbf{p}'}{2} \middle| t_{0i}(\epsilon) \middle| \frac{\mathbf{k} - \mathbf{p}}{2} \right\rangle, \quad (2)$$

where

$$\epsilon = E - \frac{\hbar^2 |\mathbf{k} + \mathbf{p}|^2}{4m}, \quad (3)$$

m is the nucleon mass and E is the incident beam energy. If we now neglect target recoil effects and make the change of variable, $\mathbf{P} = \mathbf{p} - \mathbf{q}/2$, we may write the full folding expression for the optical potential

$$\langle \mathbf{k}' | \hat{U}^{(1)} | \mathbf{k} \rangle = \frac{A-1}{A} \sum_{\alpha_i, i=n,p} \int d\mathbf{P} \langle \alpha_i | \mathbf{P} - \frac{\mathbf{q}}{2} \rangle \langle \mathcal{H}' | t_{0i}(\varepsilon) | \mathcal{H} \rangle \langle \mathbf{P} + \frac{\mathbf{q}}{2} | \alpha_i \rangle, \quad (4)$$

where $\mathbf{q} = \mathbf{k}' - \mathbf{k}$ is the momentum transfer and \mathcal{H} and \mathcal{H}' , functions of \mathbf{P} , are the relative momenta of the two active nucleons, i.e.,

$$\mathcal{H} = [\mathbf{k} - \mathbf{P} - \mathbf{q}/2]/2, \quad \mathcal{H}' = [\mathbf{k}' - \mathbf{P} + \mathbf{q}/2]/2. \quad (5)$$

If we neglect the momentum p of the struck nucleon, in Eq. (3), and take for k its on-shell value $k_0 = (2mE/\hbar^2)^{1/2}$, it follows that the required NN transition matrix should be evaluated at an energy $\varepsilon = E/2$, corresponding to free NN scattering at half the beam energy in their center-of-mass frame. This is the approximation used in this paper.

III. THE FINITE NUCLEUS MODEL

In describing the target nucleus, we do not distinguish between protons and neutrons. We take the radial parts of the single-particle wave functions $\langle \mathbf{p} | \alpha_i \rangle$ to be of harmonic oscillator (HO) form, denoted $R_{n_a l_a}(p)$, normalized such that

$$\int p^2 R_{n_a l_a}(p) R_{n'_a l'_a}(p) dp = \delta_{n_a n'_a}. \quad (6)$$

The HO parameter a , see the Appendix for details, was obtained by fitting the calculated charge densities to the available electron-scattering data.^{7,8} The corresponding target matter densities were then deduced from this same length parameter.

IV. THE OPTIMAL FACTORIZATION APPROXIMATION

For a closed-shell target nucleus, the result of the sum over the occupied states, in Eq. (4), is

$$\langle \mathbf{k}' | \hat{U}^{(1)} | \mathbf{k} \rangle = \frac{A-1}{A} \int d\mathbf{P} \langle \mathcal{H}' | \bar{t}_{01}(\varepsilon) | \mathcal{H} \rangle \rho \left[\mathbf{P} - \frac{\mathbf{q}}{2}, \mathbf{P} + \frac{\mathbf{q}}{2} \right], \quad (7)$$

where $\bar{t}_{01}(\varepsilon)$ is the spin and isospin averaged NN transition matrix⁴

$$\langle \mathcal{H}' | \bar{t}_{01}(\varepsilon) | \mathcal{H} \rangle = \bar{A}(\varepsilon, \mathcal{H}', \mathcal{H}) + \sigma \cdot \hat{n} \bar{C}(\varepsilon, \mathcal{H}', \mathcal{H}), \quad (8)$$

with σ the Pauli spin matrix for the projectile, $\hat{n} = \mathcal{H} \times \mathcal{H}' / |\mathcal{H} \times \mathcal{H}'|$, and where

$$\rho \left[\mathbf{P} - \frac{\mathbf{q}}{2}, \mathbf{P} + \frac{\mathbf{q}}{2} \right] = 4 \sum_{n_a l_a} \frac{(2l_a + 1)}{4\pi} R_{n_a l_a} \left[\left| \mathbf{P} - \frac{\mathbf{q}}{2} \right| \right] R_{n_a l_a} \left[\left| \mathbf{P} + \frac{\mathbf{q}}{2} \right| \right] P_{l_a}(\cos\theta_p). \quad (9)$$

In this expression P_{l_a} is the Legendre polynomial and θ_p is the angle between the vectors $\mathbf{P} + \mathbf{q}/2$ and $\mathbf{P} - \mathbf{q}/2$. The matrix elements of the two-body transition matrix $\langle \mathcal{H}' | \bar{t}_{01}(\varepsilon) | \mathcal{H} \rangle$ are more conveniently expressed⁹ in terms of the momentum transfer \mathbf{q} and the average of the relative momenta of the two nucleons $\mathbf{Q} = (\mathcal{H}' + \mathcal{H})/2$, that is $\bar{t}_{01}(\varepsilon, \mathbf{q}, \mathbf{Q})$. Within this notation equation (7) can be rewritten as

$$\langle \mathbf{k}' | \hat{U}^{(1)} | \mathbf{k} \rangle = \frac{A-1}{A} \int d\mathbf{P} \bar{t}_{01}[\varepsilon, \mathbf{q}, \mathbf{Q}(P)] \rho \left[\mathbf{P} - \frac{\mathbf{q}}{2}, \mathbf{P} + \frac{\mathbf{q}}{2} \right], \quad (10)$$

where the dependence of \mathbf{Q} on P has been made explicit.

The density matrix $\rho(\mathbf{P} - \mathbf{q}/2, \mathbf{P} + \mathbf{q}/2)$ is strongly peaked at $P=0$. Thus, assuming that the transition matrix \bar{t}_{01} is a slowly varying function of \mathbf{Q} , it has been suggested⁵ that these matrix elements of the transition matrix should be fixed at $\bar{t}_{01}[\varepsilon, \mathbf{q}, \mathbf{Q}(P=0)]$. This leads to the so-called optimal factorization form for the first-order optical potential

$$\langle \mathbf{k}' | \hat{U}^{(1)} | \mathbf{k} \rangle = U_{of}^c(\mathbf{k}', \mathbf{k}) + \sigma \cdot \hat{n} U_{of}^{ls}(\mathbf{k}', \mathbf{k}). \quad (11)$$

The central and spin-orbit components of the interaction are given by

$$U_{of}^c(\mathbf{k}', \mathbf{k}) = \frac{A-1}{A} \bar{A}(\varepsilon, \mathbf{q}, \mathbf{Q}/2) [A\rho(q)], \quad (12)$$

$$U_{of}^{ls}(\mathbf{k}', \mathbf{k}) = \frac{A-1}{A} \bar{C}(\varepsilon, \mathbf{q}, \mathbf{Q}/2) [A\rho(q)], \quad (13)$$

where $\mathbf{Q} = (\mathbf{k} + \mathbf{k}')/2$ is the mean of the incoming and outgoing projectile momenta and \hat{n} the unit normal to the scattering plane in the NA center-of-mass frame.

The nuclear matter density $\rho(q)$ is normalized such that $\rho(0) = 1$. Explicitly, within the HO model,

$$\rho(q) = [1 - \frac{1}{8}(qa)^2] \exp(-q^2 a^2/4), \quad (14)$$

and

$$\rho(q) = [1 - \frac{1}{4}(qa)^2 + \frac{1}{80}(qa)^4] \exp(-q^2 a^2/4), \quad (15)$$

for the ¹⁶O and ⁴⁰Ca systems, respectively.

V. THE FULL FOLDING OPTICAL POTENTIAL

In order to clarify the validity of the optimal factorization approximation described above, we will compare its predictions with those of the full folding calculations, obtained using the general method proposed by Redish and Stricker-Bauer.⁹ Defining ϕ as the angle between \mathbf{q} and \mathbf{Q} , the required matrix elements of $\bar{t}_{01}(\varepsilon)$ can be written

$$\begin{aligned} \bar{t}_{01}[\varepsilon, \mathbf{q}, \mathbf{Q}(P)] &= \bar{t}_{01}(\varepsilon, \mathbf{q}, \mathbf{Q}, \phi) \\ &= \bar{A}(\varepsilon, \mathbf{q}, \mathbf{Q}, \phi) + \sigma \cdot \mathbf{N} \bar{C}'(\varepsilon, \mathbf{q}, \mathbf{Q}, \phi), \end{aligned} \quad (16)$$

where $\mathbf{N} = (\mathbf{Q} \times \mathbf{q})/qQ$. Thus, \bar{C}' is related to the conventional spin/isospin averaged spin-orbit Wolfenstein amplitude \bar{C} , Eq. (8), according to $\bar{C}' = \bar{C}/\sin\phi$. Evaluation of the off-shell components of \bar{A} and \bar{C}' using realistic NN interactions^{1,9} shows that for NN relative momenta less than 3 fm^{-1} and $50 \text{ MeV} \leq \varepsilon \leq 200 \text{ MeV}$, they are essentially independent of the variables ε and ϕ . Therefore, in order to simplify the integration over the angular variables of \mathbf{P} , it is convenient to perform a change of integration variable (to \mathbf{Q})

$$\begin{aligned} \langle \mathbf{k}' | \hat{U}^{(1)} | \mathbf{k} \rangle &= 8 \frac{(A-1)}{A} \int d\mathbf{Q} \bar{t}_{01}(\varepsilon, \mathbf{q}, \mathbf{Q}) \\ &\quad \times \rho(\mathbf{k}-2\mathbf{Q}, \mathbf{k}'-2\mathbf{Q}) \end{aligned} \quad (17)$$

and to then fix ϕ in the scattering amplitudes \bar{A} and \bar{C}' to its on-shell value $\phi_0 = \pi/2$.

The density $\rho(\mathbf{k}-2\mathbf{Q}, \mathbf{k}'-2\mathbf{Q})$ depends only on μ , the cosine of the angle between \mathbf{Q} and $\mathbf{k}+\mathbf{k}'$. In the evaluation of the integral over \mathbf{Q} we thus choose our z axis along the direction $\mathbf{k}+\mathbf{k}'$. The full folding integral can then be reduced to the standard form

$$\langle \mathbf{k}' | \hat{U}^{(1)} | \mathbf{k} \rangle = U_{ff}^c(\mathbf{k}', \mathbf{k}) + \sigma \cdot \hat{\mathbf{n}} U_{ff}^{ls}(\mathbf{k}', \mathbf{k}). \quad (18)$$

The central component of the interaction is

$$\begin{aligned} U_{ff}^c(\mathbf{k}', \mathbf{k}) &= 8 \frac{(A-1)}{A} \int Q^2 d\mathbf{Q} \bar{A}(\varepsilon, \mathbf{q}, \mathbf{Q}, \phi_0) \\ &\quad \times \sum_{n_\alpha l_\alpha} \frac{(2l_\alpha+1)}{\pi} \mathcal{J}_{n_\alpha l_\alpha}^c, \end{aligned} \quad (19)$$

with

$$\begin{aligned} \mathcal{J}_{n_\alpha l_\alpha}^c &= 2\pi \int_{-1}^1 d\mu R_{n_\alpha l_\alpha}(|\mathbf{k}-2\mathbf{Q}|) R_{n_\alpha l_\alpha}(|\mathbf{k}'-2\mathbf{Q}|) \\ &\quad \times P_{l_\alpha}(\cos\theta_Q), \end{aligned} \quad (20)$$

where θ_Q is the angle between the vectors $\mathbf{k}'-2\mathbf{Q}$ and $\mathbf{k}-2\mathbf{Q}$.

The spin-orbit component, after performing the azimuthal integration,¹ is similarly given by the relation

$$\begin{aligned} U_{ff}^{ls}(\mathbf{k}', \mathbf{k}) &= 8 \frac{(A-1)}{A} \frac{|\mathbf{k} \times \mathbf{k}'|}{Qq} \\ &\quad \times \int Q^2 d\mathbf{Q} \bar{C}'(\varepsilon, \mathbf{q}, \mathbf{Q}, \phi_0) \\ &\quad \times \sum_{n_\alpha l_\alpha} \frac{(2l_\alpha+1)}{\pi} \mathcal{J}_{n_\alpha l_\alpha}^{ls}, \end{aligned} \quad (21)$$

where

$$\begin{aligned} \mathcal{J}_{n_\alpha l_\alpha}^{ls} &= 2\pi \int_{-1}^1 d\mu R_{n_\alpha l_\alpha}(|\mathbf{k}-2\mathbf{Q}|) R_{n_\alpha l_\alpha}(|\mathbf{k}'-2\mathbf{Q}|) \\ &\quad \times P_{l_\alpha}(\cos\theta_Q). \end{aligned} \quad (22)$$

Explicit formulas for the \mathcal{J}^{ls} and \mathcal{J}^c from the different occupied single-particle states, are presented in an appendix. Equivalent expressions for the optical potential in the case of ^{16}O have been presented by Elster *et al.*¹

VI. THE ELASTIC-SCATTERING OBSERVABLES

The optimal factorization, Eqs. (12) and (13), and the full folding expressions, Eqs. (19) and (21), for the first-order optical potential were calculated in the case of proton elastic scattering from ^{16}O and ^{40}Ca at 200 MeV, using the off-shell NN transition matrices calculated from the Paris potential.^{10,11} The target nucleus HO parameters used were $a = 1.77 \text{ fm}$ and $a = 1.95 \text{ fm}$, for ^{16}O and ^{40}Ca , respectively. These parameters provide a reasonable description of the charge form factors for small momentum transfers, typically $q \leq 2 \text{ fm}^{-1}$.

In order to isolate those effects originating from the full treatment the off-shell character of the full folding optical potential, we first neglect the proton-target Coulomb interaction in the calculation of the observables. In Figs. 1 and 2 we demonstrate that the optimal factorization calculations of the proton elastic vector analyzing power (A_y) angular distributions (dashed curves) are a good approximation to the full folding results (solid curves) for both the ^{16}O and ^{40}Ca systems. The differential cross-section angular distributions are not shown since the cross section shows very little sensi-

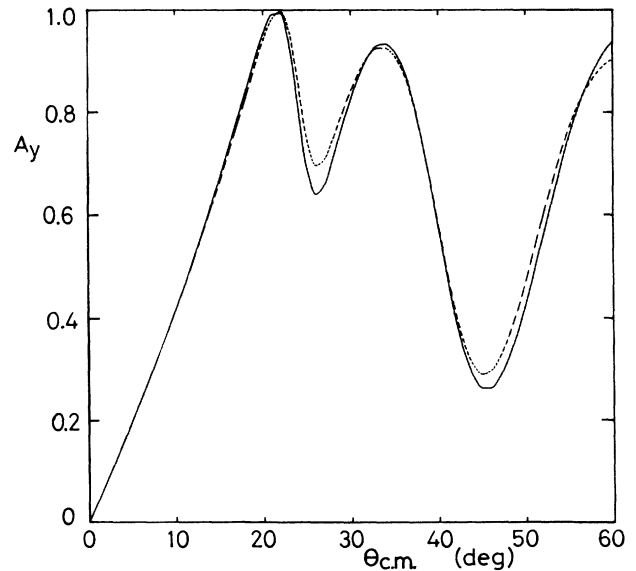


FIG. 1. Calculated vector analyzing powers A_y for p - ^{16}O elastic scattering at 200 MeV in the absence of the Coulomb interaction. The dashed and solid curves were obtained using the optimal factorization and full folding optical potentials, respectively.

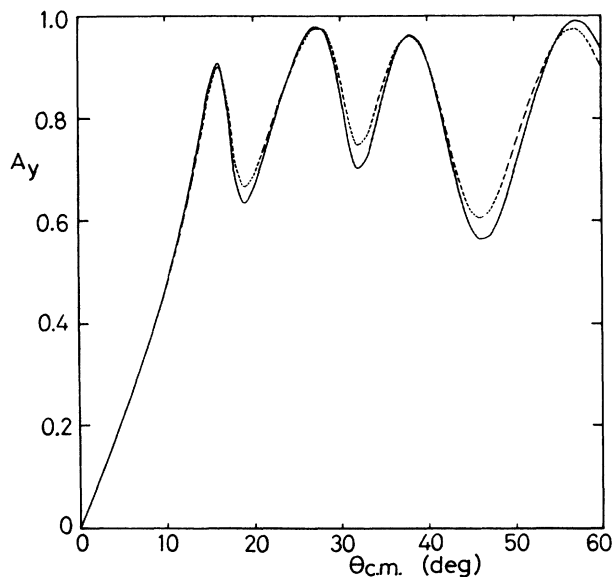


FIG. 2. Calculated vector analyzing powers A_y for p - ^{40}Ca elastic scattering at 200 MeV in the absence of the Coulomb interaction. The dashed and solid curves were obtained using the optimal factorization and full folding optical potentials, respectively.

tivity to the different approaches. Calculations were carried out, in momentum space, using the program LPOTPS.¹² In the case of ^{16}O , similar quantitative results were obtained using the NN transition matrices derived from the Bonn potential.¹ The small differences between our calculations show in the interference minima in A_y and reflect a residual sensitivity to differences in the underlying NN interactions at high momentum transfer and

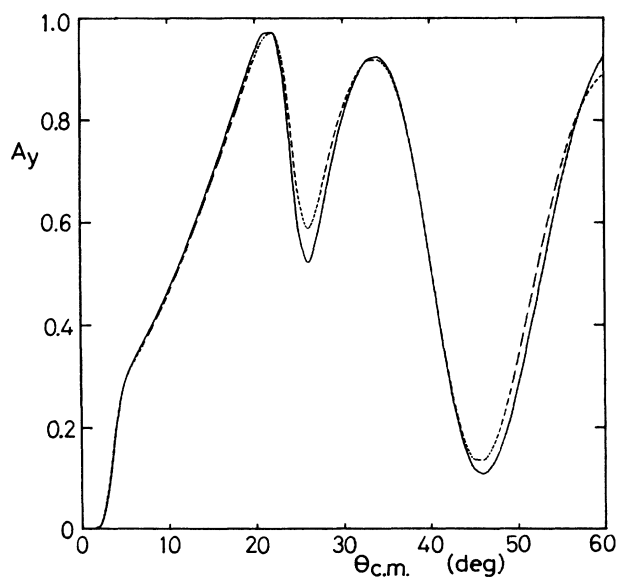


FIG. 3. As for Fig. 1, except that the Coulomb interaction is included using the subtracted momentum space method.

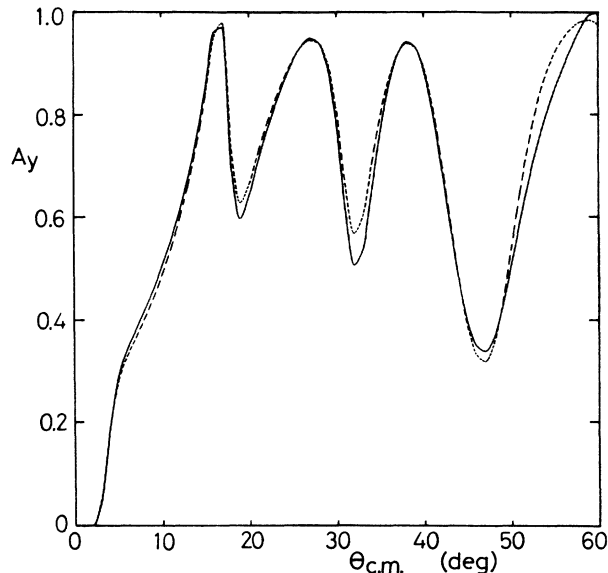


FIG. 4. As for Fig. 2, except that the Coulomb interaction is included using the subtracted momentum space method.

the slightly different values used for the single-particle HO range parameter a .

The Coulomb potential was included using the subtracted momentum space method¹³ which has been shown to produce accurate calculations of scattering observables. The Coulomb interaction was calculated from the calculated target charge densities. The cutoff radius for the Coulomb interaction, R_{cut} , used in our calculations was taken to be $R_{\text{cut}} = 10$ fm. This provided converged calculations of the proton analyzing power A_y up to center-of-mass scattering angles of 70° .

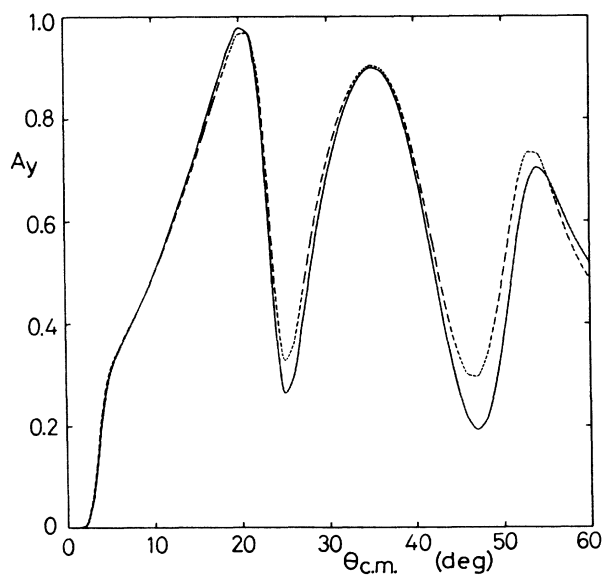


FIG. 5. As for Fig. 1 except that the Coulomb interaction is included using the technique adopted in Ref. 1.

As is shown in Figs. 3 and 4, the inclusion of the Coulomb interaction does *not* enhance the differences between the full folding (solid curves) and optimal factorization (dashed curves) calculations. We find however, that if the Coulomb interaction is included only crudely, significant changes can be introduced between the two calculations. We demonstrate this effect for the ^{16}O system in Fig. 5, in which the Coulomb interaction has been treated adopting the method used by Elster *et al.* This was referred to as Method I in Ref. 13. It consists of approximating the partial wave transition amplitudes for scattering in the presence of the Coulomb interaction by purely nuclear amplitudes, the Coulomb interaction being introduced only through the Coulomb phase factor in the partial wave expansion of the scattering amplitude. We note that, not only does this technique for treating the Coulomb interaction magnify the differences between the optimal factorization (dashed curves) the full folding results (solid curves), it also introduces a deep first interference minimum in the calculated A_y which does not arise with the more accurate Coulomb treatment. It is precisely in these interference minima that accuracy is required in order to study details of the calculated optical potentials and to investigate the need for the inclusion of higher-order terms, by comparison with the data.

In the work of Arellano *et al.*² for the $p\text{-}^{40}\text{Ca}$ system at 200 MeV, it was concluded that the optimal factorization is not a good approximation to the full folding calculations. The difference between those calculations and those presented here, other than the use of different methods for the treatment of the Coulomb interaction, is the consideration, in Ref. 2, of the momentum of the struck nucleon.

VII. CONCLUSIONS

In this paper we present calculations of elastic-scattering observables for proton scattering from ^{16}O and ^{40}Ca at 200 MeV using the first-order KMT optical potential. Calculations using the optimal factorization and full folding procedures have been carried out for both systems using consistent theoretical inputs for both systems together with an accurate treatment of the proton-target Coulomb interaction. We find that the optimal factorization procedure provides a very good approximation to the full folding results for both the ^{16}O and ^{40}Ca systems studied.

$$5\mathcal{J}_{12}^c + \mathcal{J}_{20}^c = G(k, k', x) \{ \tilde{N}_{20}^2 [\frac{9}{4} - 3\gamma(k^2 + k'^2 + 2x^2)] j_0(z) - \tilde{N}_{20}^2 6\gamma x |\mathbf{k} + \mathbf{k}'| j_1(z) \\ + \tilde{N}_{12}^2 \frac{15}{2} [(\mathbf{k} \cdot \mathbf{k}' + x^2)^2 + x^2 |\mathbf{k} + \mathbf{k}'|^2] j_0(z) + \tilde{N}_{12}^2 \frac{15}{2} x |\mathbf{k} + \mathbf{k}'| [2(\mathbf{k} \cdot \mathbf{k}' + x^2) + \gamma^{-1}] j_1(z) \} .$$

The corresponding spin-orbit integrals are

$$\mathcal{J}_{10}^{ls} = -\tilde{N}_{10}^2 G(k, k', x) j_1(z) , \\ \mathcal{J}_{11}^{ls} = -\tilde{N}_{11}^2 G(k, k', x) [(\mathbf{k} \cdot \mathbf{k}' + x^2 + \gamma^{-1}) j_1(z) + x |\mathbf{k} + \mathbf{k}'| j_0(z)] ,$$

for the 1S and 1P states and

ACKNOWLEDGMENTS

The financial support of the Instituto Nacional de Investigação Científica and the British Council (for R.C.) and the Science and Engineering Research Council (U.K.) (SERC), through research Grant Nos. GR/E/6546.3, GR/F/4105.1, and GR/F/1086.6 (for R.C.J. and J.A.T.) is gratefully acknowledged. The authors would like to thank Professor E. F. Redish for his help in providing computer programs for the evaluation of the off-shell nucleon-nucleon transition matrix. We would also like to thank Dr. Ch. Elster, for her help in comparing calculations in the case of ^{16}O , and Dr. E. D. (Tim) Cooper for many helpful discussions.

APPENDIX

In this Appendix we present explicit formulas for the harmonic-oscillator wave functions and the derived central and spin-orbit interaction integrals $\mathcal{J}_{n_a l_a}^c$ and $\mathcal{J}_{n_a l_a}^{ls}$ of Eqs. (20) and (22). Explicitly, the $R_{n_a l_a}(p)$ are

$$R_{10}(p) = \tilde{N}_{10} \exp(-p^2 a^2 / 2); \quad \tilde{N}_{10}^2 = \frac{4a^3}{\sqrt{\pi}} , \\ R_{11}(p) = \tilde{N}_{11} p \exp(-p^2 a^2 / 2); \quad \tilde{N}_{11}^2 = \frac{8a^5}{3\sqrt{\pi}} , \\ R_{12}(p) = \tilde{N}_{12} p^2 \exp(-p^2 a^2 / 2); \quad \tilde{N}_{12}^2 = \frac{16a^7}{15\sqrt{\pi}} ,$$

and

$$R_{20}(p) = \tilde{N}_{20} (a^2 p^2 - \frac{3}{2}) \exp(-p^2 a^2 / 2); \quad \tilde{N}_{20}^2 = \frac{8a^3}{3\sqrt{\pi}} .$$

For the $\mathcal{J}_{n_a l_a}^c$ and $\mathcal{J}_{n_a l_a}^{ls}$ we obtain, in the 1S and 1P states

$$\mathcal{J}_{10}^c = \tilde{N}_{10}^2 G(k, k', x) j_0(z) , \\ \mathcal{J}_{11}^c = \tilde{N}_{11}^2 G(k, k', x) [(\mathbf{k} \cdot \mathbf{k}' + x^2) j_0(z) + x |\mathbf{k} + \mathbf{k}'| j_1(z)] ,$$

where $j_0(z)$ and $j_1(z)$ are spherical Bessel functions, $x = 2Q$, $z = 2i\gamma x |\mathbf{k} + \mathbf{k}'|$, $\gamma = a^2/2$ and

$$G(k, k', x) = 4\pi \exp[-\gamma(k^2 + k'^2 + 2x^2)] .$$

The 1D and 2S contributions are best evaluated together, in which case cancellation of terms simplifies the calculation. We find

$$\begin{aligned}
5\mathcal{J}_{12}^{ls} + \mathcal{J}_{20}^{ls} = & -G(k, k', x) \left\{ \tilde{N}_{20}^2 \left[-\frac{15}{4} - 3\gamma(k^2 + k'^2 + 2x^2) \right] ij_1(z) \right. \\
& + \tilde{N}_{12}^2 15 \left[\frac{1}{2}(\mathbf{k} \cdot \mathbf{k}' + x^2)^2 + \frac{1}{\gamma}(\mathbf{k} \cdot \mathbf{k}' + x^2) + \frac{3}{4\gamma^2} + \frac{x^2|\mathbf{k} + \mathbf{k}'|^2}{2} \right] ij_1(z) \\
& \left. + \tilde{N}_{12}^2 15x |\mathbf{k} + \mathbf{k}'| \left[1 + \frac{1}{2\gamma} \right] j_0(z) - \tilde{N}_{20}^2 6\gamma j_0(z) \right\}.
\end{aligned}$$

for the 1D and 2S contributions.

*On leave from Physics Department, Instituto Superior Técnico, Lisbon, Portugal.

¹Ch. Elster, T. Cheon, E. F. Redish, and P. C. Tandy, Phys. Rev. C **41**, 814 (1990).

²H. F. Arellano, F. A. Brieva, and W. G. Love, Phys. Rev. Lett. **63**, 605 (1989).

³J. Hüfner and C. Mahaux, Ann. Phys. (N.Y.) **73**, 525 (1972); J. P. Jeukenne, A. Lejeunne, and C. Mahaux, Phys. Rev. C **16**, 80 (1977); L. Rikus and H. von Geramb, Nucl. Phys. **A426**, 486 (1984); C. Mahaux, *ibid.* **A396**, 9c (1983).

⁴A. K. Kerman, H. McManus, and R. M. Thaler, Ann. Phys. (N.Y.) **8**, 551 (1959).

⁵A. Picklesimer, P. C. Tandy, R. M. Thaler, and D. H. Wolfe, Phys. Rev. C **30**, 1861 (1984).

⁶L. Ray, Phys. Rev. C **39**, 1170 (1989).

⁷T. W. Donnelly and G. E. Walker, Phys. Rev. Lett. **22**, 1121 (1969).

⁸B. B. P. Sinha, G. A. Peterson, R. R. Whitney, I. Sick, and J. S. McCarthy, Phys. Rev. C **7**, 1930 (1973).

⁹E. F. Redish and K. Stricker-Bauer, Phys. Rev. C **35**, 1183 (1987).

¹⁰M. Lacombe, B. Loiseau, J. M. Richard, R. Vinh Mau, J. Côté, P. Pires, and R. de Tourreil, Phys. Rev. C **21**, 861 (1980).

¹¹E. F. Redish and K. Stricker-Bauer, Phys. Rev. C **36**, 513 (1987).

¹²Program LPOTPS is an extensively revised and extended version of the program LPOTP; M. J. Paez, M. E. Sagen, and R. H. Landau, Comput. Phys. Commun. **52**, 141 (1988).

¹³R. Crespo and J. A. Tostevin, *Treatment of the Coulomb interaction in momentum space calculations of proton elastic scattering*, University of Surrey report, 1989 (to appear in Phys. Rev. C).